Chemical Science International Journal

25(3): 1-6, 2018; Article no.CSIJ.28204
ISSN: 2456-706X
(Past name: American Chemical Science Journal, Past ISSN: 2249-0205)

Effect of Aluminium Metal Dosage on Surface Area, Crystallinity and Energy Band Gap of ZnO Nanostructure and Crystalline Size

O. Ojo Mathew[1], Aloba Isaac Oladele[1], Hauwa Sidi Aliyu[1*] and Salamatu Aliyu Tukur[2]

[1]Department of Chemistry, School of Science Education, Federal College of Education (Tech) Bichi, P.M.B. 3473, Kano State, Nigeria.
[2]Department of Chemistry, Faculty of Science, Kaduna State University, Kaduna State, Nigeria.

Authors' contributions:

This work was carried out in collaboration between all authors. Author OOM and HSA designed the study, performed the statistical analysis, wrote the protocol and wrote the first draft of the manuscript. Authors AIO and SAT managed the analyses of the study. Author SAT and HSA managed the literature searches. All authors read and approved the final manuscript.

Article Information

DOI: 10.9734/CSJI/2018/28204
Editor(s):
(1) Dr. Yunjin Yao, School of Chemical Engineering, Hefei University of Technology, China.
Reviewers:
(1) Kirit Siddhapara, S. V. National Institute of Technology, India.
(2) İbrahim Okur, Phyiscs, Sakarya University, Turkey.
Complete Peer review History: http://www.sciencedomain.org/review-history/27909

Original Research Article

Received 23 May 2016
Accepted 03 August 2016
Published 21 December 2018

ABSTRACT

ZnO nanocrystalline material embedded with different aluminum metal (Al) dosage was successfully prepared using the microwave synthetic technique and employing chitosan as capping agent. Temperature and power effects were monitored for best crystallinity outcome during synthetic operation with power impacting more effect on the nanocrystallinity of the ZnO as compared to the temperature. The surface area of the ZnO was observed to increase with increase in the metal dose while energy band gap decreased drastically before finally attaining a stable energy where further increment of metal was found to have no effect on the band gap of the semiconductor ZnO. Therefore for further research, this material is considered interesting in areas such as photodegradation, adsorption study, heavy metal detection and coating.

**Corresponding author: E-mail: haliyusidi.28@gmail.com;*

Keywords: Aluminum; chitosan; photo-degradation; ZnO.

1. INTRODUCTION

ZnO semiconductor nanomaterial has been observed to possess properties ranging between the bulk and its molecule with most of its physicochemical properties depending highly on particle size [1-4]. Materials in the nanoscale range have gain attention of researchers around the world due to some interesting properties such as optical and electronic properties which play an important role governing the surface atoms with increase or decrease in energy band gap resulting from electro confinement [2-5]. Thus, this surface atom makes the energy band gap determination difficult because of the in abruption of the edges of the valence and conduction bands with the ends also making the actual definition of the optical gap of the nanomaterial difficult [1]. The energy band gap in the present study has been estimated from the absorption spectrum data obtained from UV-Vis-NIR spectroscopy (UV-Vis-NIR SHIMADZU) through the linear fitting procedure. Surface area which is an important parameter in the determination of absorption ability of a material is necessary for any study involving environmental issues since there is a linear relationship between surface area and absorption of a material whereas such relationship may not exist with the particle size of the absorbent. Hence the surface area and particle of the ZnO was determined in the present study. The microwave irradiation technique is known to be a "non-conventional reaction condition" that can accelerate reaction processes in different areas of chemistry and technology [6].

2. MATERIALS AND METHODS

2.1 Materials

The precursors used for the synthesis of the ZnO embedded with aluminum metal are zinc acetate dehydrate (>99.9%), $Al(OH)_3$ (99.7%), acetic acid (≥99%), and chitosan (98%) as encap-sulating agent and double distilled water. All the chemicals were of analytical grade purchased from Merck and Sigma Aldrich.

2.2 Methods

In a sequential procedure, various range of ratio of $Zn(CH_3OO)_2.2H_2O$ and H_3COOH were dissolved in different volumes of double distilled water of 20-100 ml and agitated for 15 minutes before adding 2 ml of chitosan solution prepared by dissolving 1 g in 10 ppm acetic acid solution stirred 24 hrs and then finally transferred into a Teflon reaction vessel were it was irradiated in the Microwave oven operating at 140°C and 180W for 30 mins. The irradiated solution was then removed from the microwave and allowed to cool down naturally. Two layers were formed which were separated using microfiltration; the filtrate was washed several times with ethanol and deionised water before drying in the oven temperature of 80°C for 24 hrs.

The obtained dried nanocrystalline powders at different metal dosage were then subjected to various state characterization techniques in order to obtained information on the elemental compositions, crystallinity, surface area, energy band gap and particle shape and size of the prepared materials.

Firstly, samples phase purity and crystallinity were verified by X-ray diffraction analysis (XRD) (PAnalytical X'pert High Score software). Transmission Electron Microscopy (TEM-HITACHI H-7100) was used to confirm the samples nano-size formation and was found to correspond to the sharp peaks of the XRD analysis. Elemental composition of as-synthesized nanocomposites was obtained from X-ray fluorescence (XRF) analysis. Absorption measurement using UV-VIS was used to determine the energy band gap of the nanocrystalline Al/ZnO nanocrystalline samples by applying the Kubelka Munk plot analysis through linear fitting of the data. Finally, the specific surface area of the nanocrystalline samples was determined using the Brunauer–Emmett–Teller (BET) analysis.

3. RESULTS AND DISCUSSIONS

3.1 Crystallinity and Particle Size Determination

Spectra obtained from XRD analysis for the ZnO and Al/ZnO nanocrystalline samples are shown in Fig. 1. All the observed peaks in the images are in accordance with the International Centre for Diffraction Data (Reference Code; 98-005-2842) which belongs to the hexagonal zincite structure of ZnO. Other extra peaks observed were in accordance with the face cubic centered crystalline symmetry of Al^{2+} with ICDD indicating

the high crystallinity and purity of the prepared Al/ZnO nanocomposite with 86% crystalline phase evaluation.

The average crystallite sizes (D) of the nanocomposites were estimated by Sherrers equation using data obtained from PAnalytical X'pert High Score software

$$\lambda = 2d\sin\theta \Leftrightarrow D = k\lambda B\cos\theta \quad (1)$$

where λ=wave length 1.54 Å, k= constant 0.94, B= FWHM at 2θ, D=average crystalline size.

TEM images of the prepared nanocrystalline Al/ZnO are shown in Fig. 2 ($A_{0.00}$-$A_{0.005}$). All particle sizes where found to be below 100nm in diameter, and is in good agreement with the estimated results for average crystallite sizes from XRD spectra. The darker portions observed from the TEM micrographs of the nanocrystalline samples indicates the ZnO nanorods while the lighter spherical contrasted portions clearly indicate the Al metal attached on the surface of the ZnO semiconductor nanomaterial.

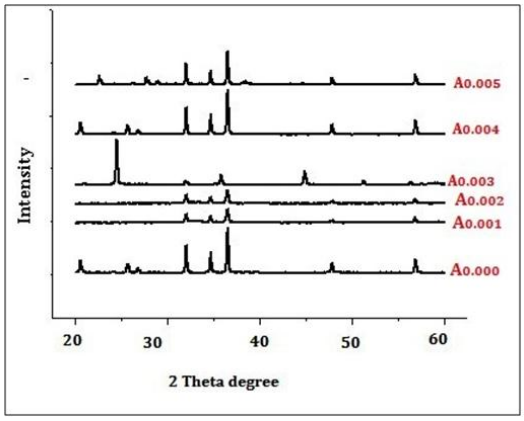

Fig. 1. Comparative XRD microgram of ZnO and different dosage 1%-5% ($A_{0.00}$-$A_{0.005}$) of Al embedded on ZnO

3.2 Surface Area Determination

Table 1 shows the composition and percentages of both main and trace elements present in the microwave prepared Al/ZnO nanocrystalline samples. It has been observed that generally, results obtained from XRF analysis depend on combination of errors contributed by the method of sample preparation and measurement of both the background intensities with peak value [7]. From the XRF analysis base on quantitative indication of analyte composition, the nanocrystalline samples were found to contain different percentage (%) compositions.

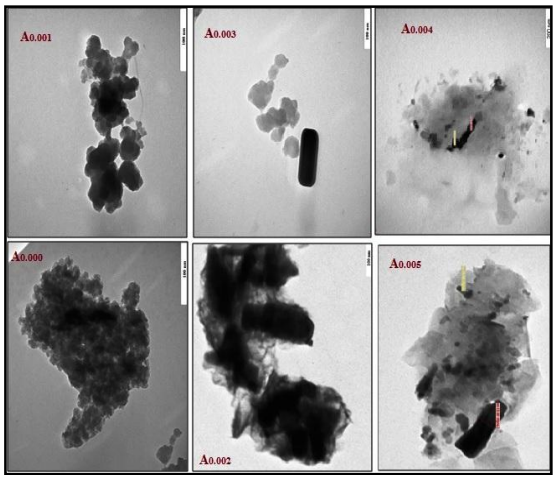

Fig. 2. TEM images of ZnO and different dosage 1-5% ($A_{0.001}$-$A_{0.005}$) of Al embedded on ZnO

The BET analysis in Table 2; showed the surface areas and pore volume of the microwave prepared Al/ZnO nanocrystalline materials at different metal dose. It was observed that embedding of aluminum metal into the matrix of the ZnO semiconductor increases both its surface area and pore volume. This observation might be as a result of the porosity of the materials which is the measure of the empty spaces in a material and is expressed as fraction of volume of empty area over the total volume, between 0 and 1, or between 0 and 100% as percentage.

3.3 Energy Band Gap Determination

The absorption data for band gap determination was measured using the UV-VIS-NIR spectrophotometer at room temperature in the wavelength of range 220-800 nm and the energy band gap absorbance edge was found to appear at (369 nm) for pure ZnO and (387 nm) for ZnO embedded with different aluminum dosage. All of which fall within the visible region. The band gap energy which is the photon energy at which transition between absorption and non absorbing behaviour takes place is determined by linear fitting of the sample absorption spectrum edge using the Kubelka Munk plot analysis which is in the transition region. As observed in Fig. 3($A_{0.00}$-$A_{0.005}$). There was

Table 1. Quantitative elemental analysis by XRF for 1-5% ($A_{0.00}$-$A_{0.005}$) Al/ZnO

I.D	Analyte	% Mass	Std. dev.	Line	Intensity (cpc/Au)
$A_{0.000}$	Zn	98.210	0.069	Zn-Ka	1895.9432
	O	1.371	0.021	O-Ka	235.0300
	N	0.110	0.008	N-Ka	16.2757
	C	0.309	0.002	C-Ka	7.0494
$A_{0.001}$	Zn	97.654	0.064	Zn-Ka	1673.7531
	O	1.271	0.014	O-Ka	129.9542
	Al	0.918	0.031	Al-Ka	15.9642
	N	0.155	0.022	N-Ka	5.0471
	C	0.002	0.002	C-Ka	7.2397
$A_{0.002}$	Zn	95.532	0.057	Zn-Ka	1595.4931
	O	1.191	0.026	O-Ka	213.0300
	Al	2.125	0.039	Al-Ka	36.2757
	N	0.042	0.023	N-Ka	8.0494
	C	0. 440	0.011	C-Ka	2.2397
$A_{0.003}$	Zn	94.114	0.052	Zn-Ka	1192.5156
	O	1.870	0.019	O-Ka	312.735
	Al	3.082	0.038	Al-Ka	98.2757
	N	0.565	0.017	N-Ka	1.0494
	C	0.069	0.010	C-Ka	0.2397
$A_{0.004}$	Zn	92.902	0.042	Zn-Ka	2091.9442
	O	1.282	0.019	O-Ka	292.0300
	Al	4.915	0.028	Al-Ka	72.3337
	N	0.069	0.014	N-Ka	9.0118
	C	0.852	0.010	C-Ka	12.7923
$A_{0.005}$	Zn	93.002	0.051	Zn-Ka	1598.1234
	O	2.171	0.023	O-Ka	135.0321
	Al	6.010	0.037	Al-Ka	122.2777
	N	0.065	0.021	N-Ka	6.0031
	C	0.852	0.012	C-Ka	1.5291

Table 2. Surface area analysis of mesoporous Al/ZnO nanomaterial from BET

Sample I.D	Surface area (m^2/g)	Total pore volume, V_t (m^3/g)	Average pore diameter Va (nm)	BHJ pore volume $V_{meso+macro}$ (m^3/g)
$A_{0.000}$	4.323	0.037	4.859	0.074
$A_{0.001}$	4.887	0.022	5.660	0.045
$A_{0.002}$	5.790	0.020	6.600	0.040
$A_{0.003}$	6.116	0.070	4.332	0.140
$A_{0.004}$	10.414	0.110	3.427	0.221
$A_{0.005}$	37.445	0.163	4.305	0.331

an observed reduction in the band gap of the prepared samples from the pure ZnO to metal embedded showing highest band gap reduction as illustrated in Fig. 3. The method used for the estimation of the band gap value was derived from the relationship between the absorption coefficient α and the incident energy of photon hv;

$$\alpha h\upsilon = (A(h\upsilon) - E_g)n \quad (2)$$

where A is a constant, E_g is the optical band gap and exponential n depends on the type of transition from n = ½ for any allowed direct transition, 2 for allowed indirect transition, 3/2 & 3 for all forbidden direct and indirect transitions respectively.

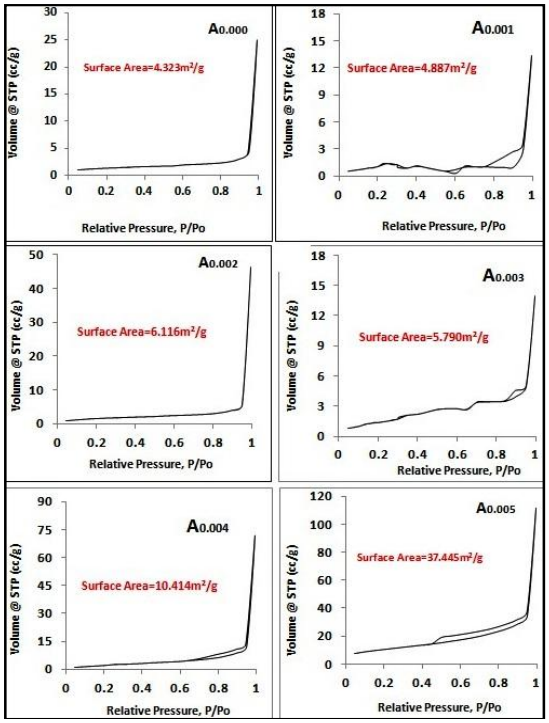

Fig. 3. BHJ adsorption pore size distribution for mesoporous surface area of ZnO ($A_{0.000}$) and Al embedded at different dosage 1-5% ($A_{0.001}$-$A_{0.005}$) on ZnO nanocrystalline samples

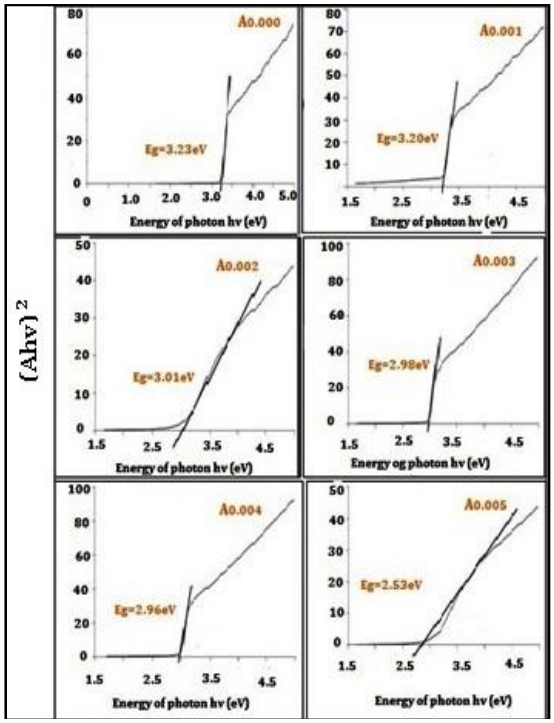

Fig. 4. Energy Band Gap Images from UV-visible spectroscopy absorption measurement for microwave prepared ZnO and Al embedded on ZnO at different dosage 1-5% ($A_{0.001}$-$A_{0.005}$)

Various plots between $(\alpha hv)^2$ against energy of photon hv were plotted as shown in Fig. 3. The observed increasingly narrowing of the band gap with the increase in aluminum metal dosage might well be as a result of many experimental synthetic factors such as the bowing effect of band gap, band formation due to impurity, increased crystallite size, and many more [8-10]. The decrease in band gap in the present study is basically due to variation in crystallite size as a result of incorporation of embedded metal into the matrix of the ZnO semiconductor. An embedment of the metal on the surface of the semiconductor which leads to decrease in optical band gap resulting to the phenomenon known as red shift which completely deviate the Burstein-Moss shift [8,9,11] was observed. Estimated band gap from the plots for the metal embedded nanocrystalline semiconductor was found to be close with the bulk ZnO, thus it can be concluded that there is no actual quantum size confinement indicating that metal localization into the matrix of the host ZnO lattice.

4. CONCLUSION

The synthesis of Al embedded onto the matrix of ZnO semiconductor is achieved using the microwave synthetic method. All the particle sizes were found to be in the nanometer (<100 nm) range and crystalline in nature. Surface area and porosity of ZnO were observed to increase with continuous increment of the Al dosage from 1-5% while the energy band gap decreased from 3.23eV to 2.63eV. It can be concluded that this material would be of interest for further research area such as degradation of waste water, coating etc.

COMPETING INTERESTS

Authors have declared that no competing interests exist.

REFERENCES

1. Ghobadi N. Band gap determination using absorption spectrum fitting procedure. International Nano Letters International Nano Letters; 2013.

2. Seong H, Jeong Bit Na P, Dong-Geun Y, Jin-Hyo B. Al-ZnO thin films as transparent conductive oxides: Synthesis, characterization, and application tests. Journal of the Korean Physical Society; 2007.
3. Wang Y, Herron N. Nanometer-sized semiconductor clusters: Materials synthesis, quantum size effects and photophysical properties. Journal of Physics Chemistry; 1991.
4. Alivisators AP. Semiconductor clusters, nanocrystals, and quantum dots. Science; 1993.
5. Peidong Y, Haoquan Y, Samuel M, Richard R, Justin J, Richard S, Nathan M, Johnny P, Rongrui H, Heon-Jin C. Controlled growth of ZnO nanowires and their optical properties. Advance Functional Material; 2002.
6. Giguere RA. Theory and application. (Hudlicky T. Edit) JAI Press Inc.; 1989.
7. Kim JK. Removal of pharmaceutical and personal care products using UV/TCNSP composites process in water PhD Research Thesis University College London; 2012.
8. Amann MC, Capasso F, Larsson A, Pessa M. Synthesis, dopant study and device fabrication of zinc oxide. New Journal of Physics; 2009.
9. Rajeswari N, Yogamalar A, Chandra B. Absorption-emission study of hydrothermally grown Al-ZnO nanostructures Journal of Alloys and Compounds; 2011.
10. Jongnavakit P, Amornpitoksuk P, Suwaboon S, Ndiege N. Preparation and activity of Cu-doped ZnO thin films by sol-gel method. Journal of Applied Surface Sci; 2012.
11. Mohajerani MS, Mazloumi M, Lak A, Kajbafvala A, Zanganeh S, Sadinezhadd SK. Self assembled zinc oxide nanostructures via a rapid microwave-assisted route. Journal of Cryst. Growth; 2008.

Peer-review history:
The peer review history for this paper can be accessed here:
http://www.sciencedomain.org/review-history/27909